GA–A22694

THEORY OF INTERNAL AND EDGE TRANSPORT BARRIERS

by
G.M. STAEBLER

OCTOBER 1997

DISCLAIMER

GA–A22694

THEORY OF INTERNAL AND EDGE TRANSPORT BARRIERS

by
G.M. STAEBLER

This is a preprint of a paper to be presented at the 6th IAEA Technical Committee Meeting US/Japan Workshop on H–Mode Physics, September 22–24, 1997, Kloster Seeon, Germany and to be published in *Plasma Physics and Controlled Fusion*.

Work supported by
the U.S. Department of Energy
under Grant No. DE-FG03-95ER54309
and Contract No. DE-AC03-89ER51114

GA PROJECTS 3726 and 3466
OCTOBER 1997

ABSTRACT

A new era of tokamak transport physics research has opened up with the discovery of a variety of internal transport barrier regimes. With suppression of some instabilities in the plasma, subdominant transport processes can be observed for the first time. In this paper, the theory of internal and edge transport barriers is reviewed with an emphasis on what is still needed in order to have a predictive transport theory of tokamak plasmas with barriers.

1. INTRODUCTION

This paper reviews the recent progress in understanding transport barriers at the edge and in the interior. In the next section, the stability mechanisms which can lead to transport barriers are discussed. The third section takes a closer look at recent progress in understanding the mechanics of E×B velocity shear suppression of transport. Section 4 reviews the status of transport barrier modeling and what is needed to have a predictive theory. The fifth section surveys new developments in H–mode theory. The poloidal momentum balance equation at the tokamak edge and the role of neutrals and viscosity are discussed. The concluding section summarizes the paper.

2. STABILITY PROPERTIES OF TRANSPORT BARRIER REGIMES

It is the aim of this section to review the known mechanisms which can lead to transport barriers by suppressing toroidal drift waves and magnetohydrodynamic (MHD) ballooning modes (kinetic, resistive, etc.). Of the many stabilizing influences on these modes, only a few can lead to dynamic bifurcations in the transport (i.e., a discontinuous jump from one stable equilibrium of the transport equations to another through an intermediate unstable state). Two mechanisms have been identified which can yield dynamic bifurcations in tokamaks: shear in the E×B velocity ($\omega_{E\times B}$) [1–5] and the Shafranov shift (α) [6,7] when the magnetic shear ($\hat{s}$) is less than a critical value ($\hat{s}_{min}$) such that the MHD ballooning modes have access to the second stable regime (i.e., there is no ideal MHD limit to the pressure gradient). A third mechanism is possible for pure ion temperature gradient modes (ITG) (also known as η_i modes) and electron temperature gradient modes (ETG) (also known as η_e modes). For these modes, the instability has a temperature gradient threshold which depends on the density gradient. This can, in principle, lead to a bifurcation driven by the particle source [8]. The trapped electron mode (TEM) and trapped ion mode (TIM) are destabilized by density gradients so a density gradient driven bifurcation is only possible near the magnetic axis, or in a highly collisional edge region, where trapped particles are absent. The three mechanisms which can lead to transport barriers, density gradients, E×B velocity shear and Shafranov shift are not independent of each other. Increasing the density gradient increases the Shafranov shift (pressure gradient) and can either increase or decrease the E×B velocity shear. Similarly, the temperature gradient affects both the Shafranov shift and the E×B velocity shear. The bifurcation which forms a transport barrier is thus multichannel in nature and can involve all three mechanisms.

In order to make full use of an internal transport barrier, it is essential to have second stable access for ideal ballooning modes. It is likely that internal transport barriers cannot penetrate into the positive shear region because of the first stable limit. This would explain the observed tendency for the leading edge of the transport barrier to track with the point of zero magnetic shear. Therefore, it is essential to control the current profile and avoid the ideal MHD boundary in order to control transport barriers. The magnetic shear $\hat{s}$ must be below the minimum value $\hat{s}_{min}$ for which an ideal MHD ballooning mode instability can exist. This also motivates the need for an accurate, full geometry, calculation of the ideal MHD boundary including E×B shear effects. Such a code has recently been developed. The ideal MHD ballooning mode boundary has been shown to be changed by E×B velocity shear [9]. The value of $\hat{s}_{min}$ is raised by E×B velocity shear.

If the plasma is resistive [10,11] or has a nonlinear anomalous hyperviscosity contributing to current diffusion [12], the pressure gradient threshold for the MHD ballooning modes can be much lower than the ideal limit. These dissipative modes will be weaker for negative magnetic shear. Even for positive magnetic shear, the transport from the instability can be greatly reduced by E×B velocity shear [12]. However, since the reduced transport would increase the pressure gradient, it is not likely that the self-consistent evolution of both the pressure gradient and $\omega_{E\times B}$ would lead to suppressed transport if the pressure gradient is in the domain of instability for ideal MHD ballooning modes. Simulations of resistive ballooning modes do show bifurcations to reduced transport when $\hat{s} < \hat{s}_{min}$ [6] or for α below the ideal stability boundary. The current diffusive ballooning mode (CDBM) can be unstable in the hot plasma core since it does not require high collisionality [12]. However, the CDBM requires a nonlinear current diffusion term. The CDBM is not a linear instability of the gyrokinetic equation.

The experimentally observed value of the E×B velocity shear is in the range of the ITG and TEM growth rates [13]. The ETG modes have much larger growth rates and, therefore, should not be stabilized by the E×B shear. The ETG modes are a good candidate for explaining the anomalous electron thermal transport within the transport barrier where the ions have neoclassical levels of thermal transport. The ETG modes can be stabilized by electron density gradients or Shafranov shifts when $\hat{s} < \hat{s}_{min}$. The ETG mode stability correlates well with the improved electron thermal transport in some plasmas with strong central magnetic shear reversal [13]. However, neoclassical levels of electron thermal transport are not observed even when the ETG mode is calculated to be linearly stable [14]. The ETG mode is also not expected to produce much particle transport according to quasi-linear theory. This contradicts the experimental observation of plasmas with neoclassical levels of transport only for the ion thermal channel [13].

This survey has just scratched the surface of the issues which need to be resolved in order to completely classify all of the various transport regimes. Much more detailed ITG and TEM linear stability results in VH–mode, high β_p and high ℓ_i modes have been reported by Rewoldt using the FULL code [15]. The NCS and ERS regimes have also been investigated comparing the E×B velocity shear to the maximum growth rate for the ITG-TEM range of wavenumbers [16]. Rewoldt has also recently investigated the effect of aspect ratio on these instabilities [17]. He finds that the TEM is strongly stabilized at small aspect ratio.

3. THE MECHANICS OF E×B VELOCITY SHEAR

Of the mechanisms which can lead to transport barriers in tokamaks, E×B velocity shear is still the least understood. This is partly due to the technical difficulty in computing the linear stability of toroidal drift waves including E×B velocity shear. It is also because of the special role that nonlinearly generated E×B flows play in the saturation of electrostatic turbulence. Both of these issues have seen recent progress towards understanding.

Waltz has shown that the nonlinear saturated fluctuation amplitude follows the trend of the growth rate of the most unstable ITG mode in the sheared slab system [18]. This holds true even though small values of $\omega_{E\times B}$ are destabilizing. When all of the ITG eigenmodes are linearly stable (including E×B shear) the turbulence is quenched. If only the torus were this simple, there would be no problem calculating the value of $\omega_{E\times B}$ needed for complete transport suppression. Unfortunately, an extensive study by Waltz [18] has not found any reliable correlation between the linear eigenvalue growth rate, including $\omega_{E\times B}$, and the point at which the turbulence is quenched in the toroidal simulations. The level of $\omega_{E\times B}$ needed to quench the toroidal ITG turbulence is generally larger than the level needed to stabilize all of the eigenvalues. This is related to the fact that the instantaneous growth rate does not vanish at all ballooning angles when the eigenvalue does because the eigenvalue is an average of instantaneously growing and damped modes. There is also a nonlinear destabilization mechanism which increases the level of $\omega_{E\times B}$ needed to quench the turbulence starting with a finite amplitude.

In order to be able to have a predictive transport model, the critical value for $\omega_{E\times B}$ must be compared to something that can be calculated routinely. A semiempirical rule has been determined [18,19] for the toroidal ITG mode simulations that the turbulence is completely quenched when $\omega_{E\times B} > \gamma_{max}$ where γ_{max} is the maximum linear growth rate of the ITG ballooning modes in the simulation computed without $\omega_{E\times B}$. The rule even holds for very small magnetic shear. This rule is found to be good to within 30% for recently improved pure ITG mode simulations [18]. Note that this rule is only good for toroidal geometry. In the sheared slab geometry, it fails. Again, the eigenvalue growth rate including $\omega_{E\times B}$ gives the stability point in the sheared slab. This rule has been widely used to analyze internal transport barrier experiments and is found to work well in many cases. An example is shown in Fig. 1 from Ref. [16]. For this DIII–D WNS discharge, $\omega_{E\times B} > \gamma$ across the whole plasma. This agrees with the neoclassical level of ion thermal transport found by power balance analysis over the entire radius.

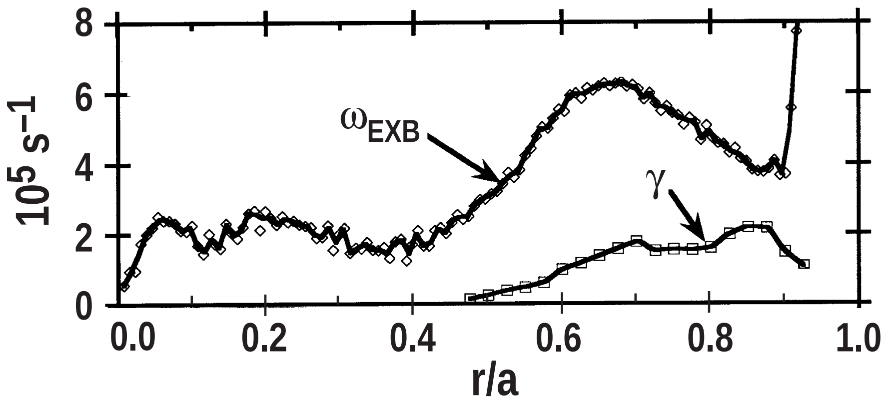

Fig. 1. Results for γ and $\omega_{E\times B}$ verses r/a for DIII–D WNS discharge 84713 at t = 2.08 s with γ for electrostatic toroidal drift mode with carbon and Maxwellian beam, for $k_\theta\ \rho_i$ = 0.49. $\omega_{E\times B}$ is from measured poloidal and toroidal rotation, temperature and density of fully stripped carbon impurity from Ref. [16].

The first theories of the suppression of turbulence by velocity shear predicted that the mechanism was a nonlinear decorrelation [3,4]. This line of theory progressed from electric fields [1–3] as the stabilizing factor, to slab E×B velocity shear [4] and finally the toroidal form of $\omega_{E\times B}$ [20,21].

$$\omega_{E\times B} = \frac{R B_\theta}{B} \frac{\partial}{\partial r}\left(\frac{E_r}{R B_\theta}\right) , \qquad (1)$$

$$E_r = U_{I\phi} B_\theta - U_{I\theta} B_\phi + \frac{1}{Z_I e n_I} \frac{d P_I}{d r}$$

where R is the major radius, B the total magnetic field, B_θ the poloidal magnetic field and E_r the radial electric filed. Whereas much progress has come from this work in resolving the correct form for $\omega_{E\times B}$, the issue of what to compare it to has not been settled. The decorrelation theory yields an approximate formula for the ratio of the diffusivity with ($D_{E\times B}$) and without (D_0) $\omega_{E\times B}$ [22].

$$D_{E\times B}/D_0 = 1/[1 + (\omega_{E\times B}/\gamma_{norm})^n] \quad , \qquad (2)$$

$$\gamma_{norm} = C\, \Delta k_r^2\, D_0\, \Delta k_r/\Delta k_\theta \quad , \qquad (3)$$

where C is a constant. The Biglari, et al., model [4] is recovered in the large $\omega_{E\times B}$ limit if C = 4 and n = 2/3. The Shaing, et al., model [3] has C = 1 and n = 2.

The problem with this formula is that the nonlinear turbulence diffusivity D_0 and the radial and poloidal wavenumber spectral widths (Δk_r, Δk_θ) are all determined in the absence of E×B velocity shear and cannot be calculated in a routine way. If one has to perform nonlinear turbulence simulations for each plasma, then the formula has no practical use. The ratio $D_{E\times B}/D_0$ also cannot be measured because the calculation assumes that everything accept $\omega_{E\times B}$ is held fixed while $\omega_{E\times B}$ is varied. This is impossible to accomplish experimentally since the profiles steepen after the barrier forms. In principle, the formula can be tested with numerical simulations where the profile gradients are held fixed. The thermal diffusivity calculated from 3D nonlinear simulations of toroidal ITG modes with adiabatic electrons was used by Waltz [18] for D_0. Using the decorrelation formula [Eq. (2)], it was found that only a very small (<10%) reduction in the turbulent diffusivity was predicted at the value of $\omega_{E\times B}$ needed to quench the fluctuations in the simulations for both the Biglari et al., and Shaing et al. models. This suggests that the nonlinear decorrelation mechanism does not play a major role in the suppression of the turbulence seen in the simulations. The decorrelation theory also does not capture the difference between slab and toroidal geometry seen in the simulations.

A similar formula to Eq. (2) with n=2 has been derived for the CDBM theory [12]. The shearing rate normalization γ_{norm} is proportional to the poloidal Alfvén speed divided by the minor radius. The CDBM has a scale length of order of the collisionless skin depth. Even though these frequency and length scales are quite different than the ITG mode, the value of $\omega_{E\times B}$ needed to effect the transport is within the experimental range due to a magnetic shear dependent factor of order 24 reducing γ_{norm}. Since the CDBM is predicted to be suppressed but not extinguished by $\omega_{E\times B}$, it is a candidate for explaining the observed density fluctuations within the transport barrier.

4. TRANSPORT BARRIER MODELING

Phenomenological transport models have been successful at reproducing the qualitative features observed in both edge and internal transport barriers. It is ironic that one of the earliest bifurcation models predicted that the transport barrier formed first at the edge but would continue to expand inward as the heating power was increased [5]. It was only later that the edge particle source was shown to localize the barrier to the edge [23] and the transition to VH–mode with a core transport barrier was understood [24]. The success of simple models is due to the use of $\omega_{E\times B}$ as a control parameter for the bifurcation to reduced transport. The dependence of the location and width of the transport barrier on the heating, fueling, and momentum source profiles was illuminated by this work. This knowledge was exploited to predict the existence of a discharge with a core transport barrier and an L–mode edge [25] not unlike the L–mode edge NCS plasmas. The ultimate H–mode (UH–mode following in the line of H, VH [26]) with suppressed transport across the whole plasma was also anticipated by modeling [5,24] before it was realized in DIII–D [27].

Generic properties shared by all bifurcation models, like hysterises and limit cycle oscillations, explain the phenomenology of dithering L/H transitions [28]. The mathematics of phase transitions has been put to use to analyze the propagation of the leading edge of a transport barrier [29] in a supercritical uniform plasma. This free propagation is faster than the expansion of the barrier in the experimental situation of a nonuniform plasma. In a nonuniform plasma, the critical value of the power flux density needed for the bifurcation to reduced transport varies in space (the criticality profile). The power flux density at the leading edge of the barrier rises as the rate of stored energy increase behind the barrier slows. The barrier expands up the gradient of the criticality profile, either inward [24] or outward [30–32], as the power flux density at the leading edge rises. Recent work has studied the role of the critical E×B shear profile on the formation, location, and the dynamics of internal transport barriers [30,31]. The interplay between diamagnetic, poloidal and toroidal velocity contributions to the electric field in internal transport barriers has also been studied [32]. Efforts to put more of the physics of the underlying instabilities has enabled predictions of power threshold scaling [30,31] and shown how a critical temperature gradient length in the growth rate can extend the width of an internal transport barrier [32]. These simple models will continue to bear fruit especially in the area of testing methods for external control. A particularly promising method is the use of radio frequency waves as a localized momentum source [33]. Transport barriers have already been observed at the absorption layer in experiments with ion Bernstein waves [34]. Other waves need to be investigated to find the theoretically most efficient and practically most reliable method. Moving beyond phenomenology, the challenge ahead is to develop predictive transport models which include the physics needed to reproduce the rich variety of plasmas with some degree of transport suppression.

Transport models have been developed which are reasonably accurate at reproducing the temperature profiles and global confinement of L–mode plasmas. If the pedestal temperature is taken as a boundary value, these same models work for H–modes. The E×B velocity shear has been incorporated into three of these models to date. The first was the GLF23 model [35]. Then the IFS-PPPL model [36] and the CDBM model [37]. The first two are based on ITG-TEM physics but differ significantly in the details.

The impact of the E×B velocity shear is not large for L–mode or H–mode core plasmas but it is essential in order to model a transport barrier. An example of a good agreement between the GLF23 model [35] and an NCS plasma with an internal transport barrier is shown in Fig. 2(a). If the E×B velocity shear is neglected, the transport barrier disappears [as shown in Fig. 2(b)] even though the negative magnetic shear and Shafranov shift are kept at their experimental values. The electron thermal transport in the barrier region (r/a < 0.3) is only from the ETG modes. If the ETG modes are turned off, the electron temperature predicted by the model rises way off scale [Fig. 2(a) dotted curve] inside of the barrier since only electron neoclassical transport is left. This was a case where the computed E×B shear was close to the experimental value measured. The E×B shear was computed in the GLF23 model using a formula for the neoclassical main ion poloidal velocity [38]. The measured toroidal velocity of carbon was corrected to the main ion velocity also using a neoclassical formula [38]. In this particular case, there was pretty good

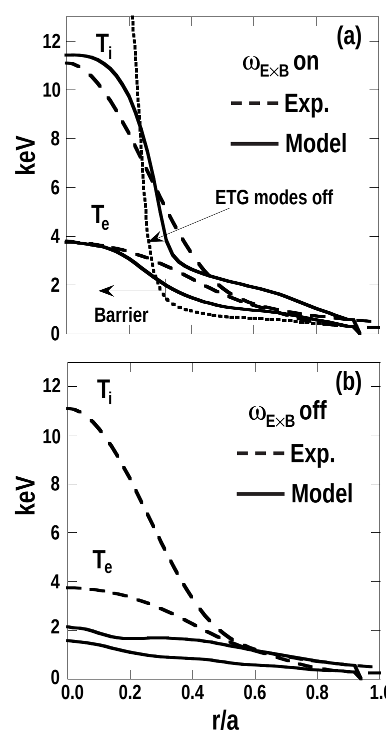

Fig. 2. Radial profile of the measured (dashed) ion and electron temperature profiles and the temperature profiles computed from the GLF23 model (solid) including E×B velocity shear (a) and without it (b) [35].

agreement with the measured $\omega_{E\times B}$. However, this is not usually the case [39]. Usually the agreement between the neoclassical carbon poloidal rotation computed with the NCLASS code [40] and the value measured is rather poor. This typically poor agreement can have a large impact on the $\omega_{E\times B}$ which must be computed in a predictive transport code. When there is no external toroidal torque, the poloidal rotation is particularly important. There are many possible reasons why the neoclassical calculation fails. First, the fast beam ion content of the central plasma is large in NCS plasmas and the beam ions are not included in the NCLASS calculation. It has been pointed out by Ohkawa that the beam ions can generate poloidal pressure asymmetries [41]. Second, the toroidal velocity is large and the impurity density may be higher on the outboard side due to centrifugal forces [42] which are known to affect neoclassical transport. Third, only one impurity species is measured and included in the calculation and only the fully stripped charge state of this one impurity. Fourth, the orbit squeezing factor was included but there are other corrections to neoclassical theory since the pressure gradient length is comparable to the poloidal gyroradius [43]. The damping of poloidal rotation can also be affected by large diamagnetic velocities [2]. If the poloidal velocity before the bifurcation is determined by standard neoclassical theory in the banana regime, then it cancels most of the temperature gradient contribution from the diamagnetic velocity in the electric field. This makes the density gradient a much stronger leverage for increasing $\omega_{E\times B}$ than the temperature gradient [32].

The transport that is left in a plasma with large $\omega_{E\times B}$ is not as well modeled as the L–mode. As discussed in Section 2, the observed richness of combinations of suppressed and anomalous transport channels is not yet categorized in terms of the properties of fundamental instabilities. Even the neoclassical theory of ion thermal transport appears to need revision downward near the magnetic axis [13]. There is controversy at present as to the proper treatment of ion orbits which pass through the magnetic axis [44,45]. The background level of transport has an impact on the bifurcation threshold, the speed of the transition, and even the existence of a bifurcation [24].

With these daunting challenges to overcome before a complete predictive transport model is possible, let us not lose sight of the fact that it is a great accomplishment that theoretical models can predict L–mode temperature profiles at all. After all, the L–mode is the worst case with all of the instabilities active and strongly coupled. The fact that models based on one or another instability work nearly as well [46] is probably because all of the models have similar scaling properties. The rich variety now showing up in enhanced confinement regimes should actually accelerate our progress in developing and testing transport models as the unique properties of the fundamental instabilities are uncovered.

5. BACK TO THE EDGE

Until now, this paper has focused on internal transport barriers. Of course, much of the physics is the same at the plasma edge. There are, however, some special properties of the edge which affect the transport barrier threshold and dynamics and make the edge bifurcation more complicated than the internal transport bifurcation. One of the main differences is the two-dimensional nature of the tokamak boundary. The poloidal location of the axisymmetric limiter or divertor has a large impact on the H–mode threshold. In order to fully account for the poloidal variation of the neutral density and radiation distribution and the neoclassical grad-B drift effects [47], a two-dimensional transport code is required. Modeling of a two-dimensional H–mode transition with self-consistent electric fields has not yet been attempted.

Progress has been made by Carlstrom [48] in modeling the impact of the ion grad-B drift and sawtooth heat pulses on the magnetic field scaling of the H–mode power threshold. The intrinsic scaling without these influences is predicted to be much weaker. This is supported by the scaling of double-null plasmas, which should have no grad-B drift effect due to their up/down symmetry, and which show a weak magnetic field scaling.

The role of the poloidal velocity in the bifurcation to H–mode continues to be a point of difficulty. The poloidal velocity is an important contributor to the total electric field [Eq. (1)]. All of the transport channels, particle, energy, toroidal and poloidal momentum need to be included, but it is the poloidal momentum which is the most controversial. Different researchers have focused on different terms in the poloidal momentum balance equation (or ignored it altogether) leading to a variety of bifurcation mechanisms. All of the important physics has, I believe, been identified and a complete ion poloidal momentum balance equation can be written down in a symbolic fashion (neglecting geometrical factors) as

$$dU/dt + (\Gamma^A dU/dr + d\Pi^A/dr)/m_i\, n_i + \nu^{NCL}(U - U^{NCL}) + \nu^{CX}U - \nu^{RSD}U = S \quad . \quad (4)$$

Here S represents the external torques, U is the poloidal velocity, U^{NCL} is the neoclassical poloidal velocity driven primarily by the ion temperature gradient, m_i is the ion mass and n_i is the ion density. The remarkable thing about this equation is that every term but the charge exchange neutral damping (ν^{CX}) has been shown to be able to yield a bifurcation.

The convective derivative can cause a Stringer spin up instability if the radial flux (Γ^{A}) is poloidally asymmetric [49]. The anomalous viscous stress (Π^{A}) can yield bifurcated states through the E×B velocity shear dependence [50]. The neoclassical poloidal damping (ν^{NCL}) reduction at large velocity gives multiple states [2] and the Reynolds stress dynamo (ν^{RSD}) can trigger a phase transition driven by turbulent flows [51]. It is important to remember that a bifurcation to reduced energy and particle transport will occur even without the aid of the poloidal velocity through the diamagnetic contribution to $\omega_{E\times B}$ [23]. However, the threshold for the bifurcation can be influenced by the poloidal velocity, and there is consistent evidence that the measured change in the poloidal velocity of the impurity leads the transition and occurs on a timescale which is faster than the changes in the temperature and density profiles [52]. Even though the impurity poloidal velocity is not the same as the main ions [38], the difference depends upon the density and temperature gradients which are not changing as quickly.

Each of these bifurcation mechanisms is well established and could, in principle, occur under the right conditions. In the case of bias probe induced bifurcations, it is clear from careful modeling that the neoclassical damping reduction plays a central role [53]. The ion orbit loss current [2] could drive a bifurcation at the edge of unbiased tokamaks but the observed main ion poloidal velocity has the opposite sign [54] to the ion orbit loss torque so other effects are dominant. It is possible that there is a short (<3 ms) period where the main ion velocity changes direction just inside of the separatrix. The time resolution and fiducials for the main ion poloidal velocity cannot resolve this issue at present. A careful study of the poloidal velocity profiles for the main ions and fully stripped carbon has shown that the charge exchange neutral damping is important for the main ions [55]. A reasonable fit (adjusting the unknown neutral density profile) to the main ion data is shown in Fig. 3(a) with only neoclassical and charge

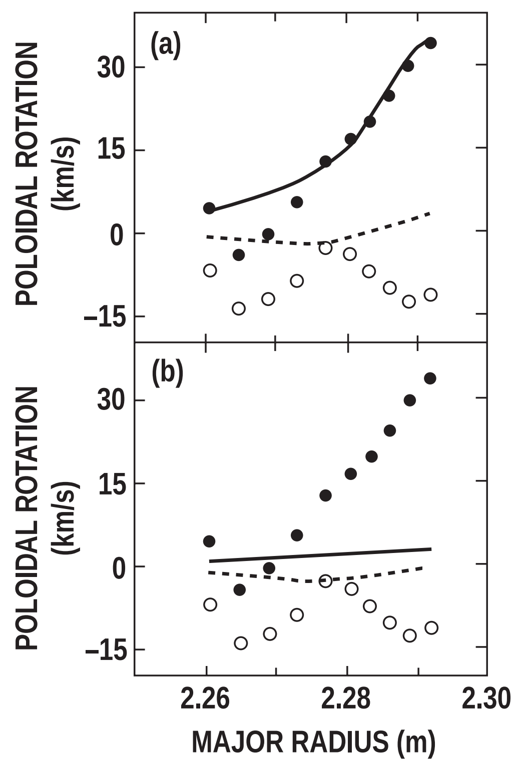

Fig. 3. Measured (symbols) poloidal velocity of the main helium ions (full) and carbon ions (open) for a DIII–D helium plasma. The computed poloidal velocity of the main ions (solid) and impurity ions (dashed) is shown from a two ion neoclassical calculation including charge exchange friction with neutral atoms (a) and without the charge exchange friction (b). The neutral density profile was adjusted to obtain a good fit [55].

exchange terms [55]. The fit for the carbon is not very good but only the fully stripped charge state was included in the neoclassical calculation. The parallel flows, which cancel the electric field and diamagnetic contribution to the poloidal rotation in standard neoclassical theory, are damped by charge exchange with neutrals. The resulting poloidal velocity tends to oppose the diamagnetic velocity [56]. This analysis uses the measured toroidal velocity.

Although the extended neoclassical theory with charge exchange [55,56] works reasonably well, it does not explain why the poloidal velocity would change faster than a change in the profiles or neutral density. It also does not satisfy the boundary condition requirements for the transition from closed to open field lines which has been emphasized by Rozanski and Tendler [57]. The flows on the open field lines of the scrapeoff layer (SOL) are determined by the positive radial electric field and particle balance. The SOL electric field is positive because of the electrostatic sheath at the end plates ($e\phi/T_e = 3$ for floating plates) and the radial temperature variation $E_r = -d\phi/dr = -(3/e)\, dT_e/dr$. If the material surface in contact with the plasma is axisymmetric, the poloidal flow in the SOL is determined by particle balance and the toroidal flow by radial force balance and E_r. On the closed flux surfaces far from the separatrix, the neoclassical poloidal damping (ν^{NCL}) dominates and the poloidal velocity is neoclassical (U^{NCL}). These two boundary conditions for the poloidal velocity do not match, in general, and a transition region is needed. A second order differential term is needed in order to bridge these two boundaries. This is supplied by the anomalous viscous stress (Π^A) term. Thus, a viscous poloidal velocity shear layer develops near the last closed flux surface. The width of this layer can be estimated by writing the poloidal velocity part of the viscous stress term in Eq. (4) as $m_i\, n_i\, \mu\, U_\theta/L^2$ where μ is the anomalous momentum diffusivity. Balancing this against the linear damping terms in Eq. (4) gives the estimated poloidal velocity gradient length as $L \sim (\mu/\nu)^{1/2}$ where ν is the sum of all of the linear damping rates. Now consider Fig. 4 which shows the radial profiles of the measured main ion poloidal velocity (a) and radial electric field (b) 7 ms before and 3 ms after the L/H transition [54]. It is clear that in L–mode, the main ion poloidal velocity gradient length just inside of the separatrix is much larger than it is in H–mode. This is consistent with a reduction in the anomalous viscosity in H–mode as would be expected from the E×B velocity shear. It is not consistent with a reduction in the linear damping. Thus, the breakdown of neoclassical damping or the change in sign of the net damping as required by the Reynolds stress dynamo theory do not appear to be consistent with the main ion rotation behavior if the anomalous viscous stress is included. The main ion poloidal velocity is not large enough in the plasma of Fig. 4(a) to be in the regime where the neoclassical damping is reduced even in the early H–mode [58] . Note that the poloidal flow in the SOL plays an important role in this theory since the mismatch between the open and closed field line solutions sets up the shear layer. External control of the SOL flow by divertor biasing [59] or puffing at one end and pumping the other would be expected to change the power threshold for the H–mode.

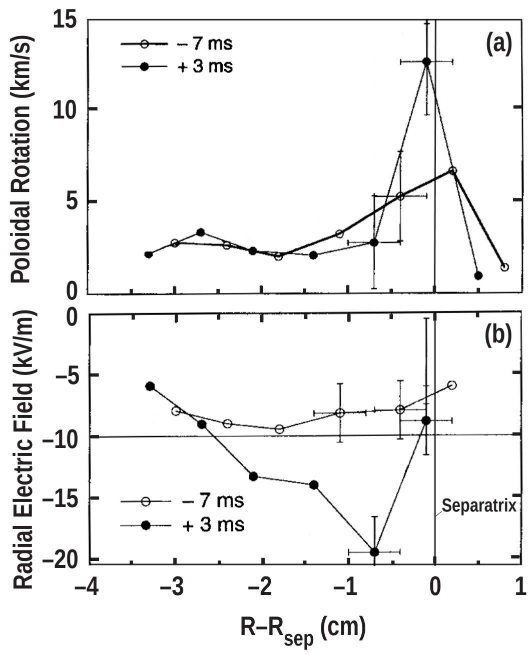

Fig. 4. Main ion (helium) poloidal rotation (a) and radial electric field profile (b) from force balance using all measured velocities and profiles from main ions. Profiles shown are 7 ms before (full) and 3 ms after (open) the transition from L– to H–mode [54].

6. SUMMARY

Because of the intense experimental and theoretical effort to understand the H–mode physics, the basic E×B shear suppression paradigm, and even the phenomenological transport models were directly applicable to the new experimental regimes with internal transport barriers (NCS, ERS, etc.). Internal transport barriers have brought much more than record performance to tokamaks, they have enabled experiments to probe the substructure of turbulence by turning off some of the instabilities. We have just begun to exploit this new ability but it has already revealed the inadequacy of existing transport models to predict the rich variety found in the new confinement regimes.

Recent work on the linear gyrokinetic stability of internal transport barrier regimes was reviewed. Although there are some promising correlations, the expectations of quasi-linear transport do not always agree with the experiments. Real progress here will probably only come from nonlinear simulations. The ability to form plasmas with a reduced spectrum of unstable modes will facilitate the comparison between nonlinear simulations and experiments.

A lot of progress has been made in understanding the mechanics of the E×B shear suppression process [18]. The global form of Waltz's rule [18,19] for complete suppression of turbulence ($\omega_{E\times B} > \gamma_{max}$) has been successfully applied to many internal transport barrier discharges. A major obstacle to predictive transport barrier models is that the neoclassical theory for poloidal rotation and transport have been found to not agree with experiment in the suppressed transport region.

The old problem of the poloidal momentum balance equation and its role in H–mode has still not been completely resolved. Since many of the influences on the edge are two dimensional, the use of poloidally averaged equations is questionable. Full two-dimensional modeling of the H–mode transition is a very complex problem so a simpler near term model is needed.

An exciting new era in tokamak transport research has begun. Transport barrier experiments can now probe the substructure of tokamak turbulence. Rapid progress in understanding the physics of transport in tokamak plasmas is expected to result from the exploration of this new territory.

ACKNOWLEDGMENTS

Thanks are due to Drs. Ron Waltz, Kimitaka Itoh, Fred Hinton and Keith Burrell for comments and suggestions. This work supported by the U.S. Department of Energy under Grant No. DE-FG03-95ER54309 and Contract No. DE-AC03-89ER51114.

REFERENCES

[1] Itoh, S.I., and Itoh, K., 1988 in *Phys. Rev. Lett.* **60**, 2276.

[2] Shaing, K.C., and Crume, E.C., 1989 in *Phys. Rev. Lett.* **63**, 2369.

[3] Shaing, K.C., Lee, G.S., Carreras, B.A., Houlberg, W.A., and Crume, Jr., E.C., 1989 in *Plasma Phys. and Contr. Nucl. Fusion Research* (Proc. 12th Int. Conf. Nice, 1988), (International Atomic Energy Agency, Vienna) Vol. 2, p. 13; Shaing, K.C., Crume, Jr., E.C., and Houlberg, W.A., 1990 *Phys. Fluids B* **2**, 1492.

[4] Biglari, H., Diamond, P.H., and Terry, P.W., 1990 in *Phys. Fluids B* **2** (1990) 1.

[5] Hinton, F.L., 1991 in *Phys. Fluids B* **3**, 696.

[6] Drake, J.F., Lau, Y.T., Guzdar, P.N., Hassam, A.B., Novakovski, S.V., et al., 1996 in *Phys. Rev. Lett.* **77**, 494.

[7] Beer, M.A., Hammett, G.W., Rewoldt, G., Synakowski, E.J., and Zarnstorff, M.C., 1997 in *Phys. Plasmas* **4**, 1792; Beer, M.A., and Hammett, G.W., 1995 *Bull. Am. Phys. Soc.* **40**, 1733.

[8] Staebler, G.M., “Density Gradient Driven Transport Bifurcation,” in preparation.

[9] Miller, R.L., Waelbroeck, F.L., Hassam, A.B., and Waltz, R.E., 1995 in *Phys. Plasmas* **2**, 3676; Miller, R.L., Lin-Liu, Y.R., Osborne, T.H., and Taylor, T.S., “Ballooning Mode Stability for Self-Consistent Pressure and Current Profiles at the H–Mode Edge,” in *Plasma Phys. and Contr. Nucl. Fusion Research* (Proc. IAEA Tech. Committee Mtg. US/Japan Wkshp. on H–Mode Physics, September 1997, Kloster Seeon, Germany), (IAEA, Vienna) to be published.

[10] Rogers, B.N., and Drake, J.F. “Electromagnetic Turbulence and Spontaneous Transport Barrier Formation in Tokamaks,” in *Plasma Phys. and Contr. Nucl. Fusion Research* (Proc. IAEA Tech. Committee Mtg. US/Japan Wkshp. on H–Mode Physics, September 1997, Kloster Seeon, Germany), (IAEA, Vienna) to be published.

[11] Scott, B.D., “Three Dimensional Computation of Drift-Alfven Turbulence,” in *Plasma Phys. and Contr. Nucl. Fusion Research* (Proc. IAEA Tech. Committee Mtg. US/Japan Wkshp. on H–Mode Physics, September 1997, Kloster Seeon, Germany), (IAEA, Vienna) to be published.

[12] Itoh, S.I., Itoh, K., Fukuyama, A., and Yagi, M., 1994 in *Phys. Rev. Lett.* **72**, 1200; Fukuyama, A., Itoh, K., Itoh, S-I., Yagi, M., and Azumi, M., 1995 in *Plasma Phys. Control. Fusion* **37**, 611.

[13] Greenfield, C.M., Schissel, D.P., Stallard, B.W., Lazarus, E.A., Navratil, G.A., et al., 1997 in *Phys. Plasmas* **4**, 1596.

[14] Schissel, D.P., Greenfield, C.M., DeBoo, J.C., Lao, L.L., Lazarus, E.A., et al., to be published in Proc. 16th IAEA Fusion Energy Conf., October 1996, Montreal, Canada, paper FI-CN-64/A5-3.

[15] Rewoldt, G., Lao, L.L., and Tang, W.M., 1996 in *Phys. Plasmas* **3**, 4074.

[16] Rewoldt, G., Lao, L.L., and Tang, W.M., 1997 in *Phys. Plasmas* **4**, 3293.

[17] Rewoldt, G., Tang, W.M., Kaye, S., and Menard, J., 1996 in *Phys. Plasmas* **3**, 1667.

[18] Waltz, R.E., "Theory and Simulation of Rotational Shear Stabilization," in Special Issue Plasma Phys. (39th Annual Mtg. Division of Plasma Phys., November 1997, Pittsburgh, Pennsylvania) to be published.

[19] Waltz, R.E., Kerbel, G.D., Milovich, J., and Hammett, G.W. 1995 *Phys. Plasmas* **2**, 2408; 1994 *Phys. Plasmas* **1**, 2229.

[20] Shaing, K.C., 1994 in *Phys. Plasmas* **1**, 219.

[21] Hahm, T.S., and Burrell, K.H., 1995 in *Phys. Plasmas* **2**, 1648.

[22] Zhang, Y.Z., and Mahajan, 1992 in *Phys. Fluids B* **4**, 1385.

[23] Hinton, F.L., and Staebler, G.M., 1993 in *Phys. Fluids B* **5** , 1281.

[24] Staebler, G.M., Hinton, F.L., Wiley, J.C., Dominguez, R.R., Greenfield, C.M., et al., 1994 in *Phys. Plasmas* **1**, 909.

[25] Staebler, G.M., Hinton, F.L., and Wiley, J.C., 1996 in *Plasma Phys. Contr. Fusion* **38**, 1461.

[26] Jackson, G.L., private communication.

[27] Lazarus, E.A., Navratil, G.A., Greenfield, C.M., Strait, E.J., Austin, M.E., et al., 1996 in *Phys. Rev. Lett.* **77**, 2714.

[28] Itoh, S-I., Itoh, K., Fukuyama, A., and Miura, Y., 1991 in *Phys. Rev. Lett.* **67** 2485.

[29] Lebedev, V.B., and Diamond, P.H., 1997 in *Phys. Plasmas* **4**, 1087; Diamond, P.H., Lebedev, V.B., Newman, D.E., and Carreras, B.A., 1995 in *Phys. Plasmas* **2**, 3685.

[30] Newman, D.E., Carreras, B.A., Lopez-Bruna, D., Diamond, P.H., and Lebedev, V.B., "Dynamics and Control of Internal Transport Barriers in Reversed Shear Discharges," to be published in *Phys. Plasmas*; Diamond, P.H., Lebedev, B.V., Newman, D.E., and Carreras, B.A., "Dynamics of Core Transport Barriers," in *Plasma Phys. and Contr. Nucl. Fusion Research* (Proc. IAEA Tech. Committee Mtg. US/Japan Wkshp. on H–Mode Physics, September 1997, Kloster Seeon, Germany), (IAEA, Vienna) to be published.

[31] Diamond, P.H., Lebedev, V.B., Newman, D.E., Carreras, B.A., Hahm, T.S., et al., 1997 in *Phys. Rev. Lett.* **78**, 1472.

[32] Staebler, G.M., Waltz, R.E., and Wiley, J.C., 1997 in *Nucl. Fusion* **37**, 287.

[33] Diamond, P.H., Phillips, C.K., "On the Control of Transport Barriers by RF Waves," in *Plasma Phys. and Contr. Nucl. Fusion Research* (Proc. IAEA Tech. Committee Mtg. US/Japan Wkshp. on H–Mode Physics, September 1997, Kloster Seeon, Germany), (IAEA, Vienna) to be published.

[34] Ono, M., 1993 in *Phys. Fluids B* **5**, 241.

[35] Waltz, R.E., Staebler, G.M., Dorland, W., Hammett, G.W., Kotschenreuther, M., et al., 1997 in *Phys. Plasmas* **4**, 2482.

[36] Dorland, W., Kotschenreuther, M., Liu, Q.P., Beer, M.A., and Hammett, G.W., "3D Simulations of Tokamak Plasma Turbulence: Experimental Tests and Predictions," in Proc. ISPP/Wkshp. on Theory of Fusion Plasmas, August 1996, Varenna, Italy to be published.

[37] Fukuyama, A., Itoh, S-I., Yagi, M., and Itoh, K., "Transition to an Enhanced Internal Transport Barrier," in *Plasma Phys. and Contr. Nucl. Fusion Research* (Proc. IAEA Tech. Committee Mtg. US/Japan Wkshp. on H–Mode Physics, September 1997, Kloster Seeon, Germany), (IAEA, Vienna) to be published.

[38] Kim, Y.B., Diamond, P.H., and Groebner, R.J., 1991 in *Phys. Fluids B* **3**, 2050.

[39] Baylor, L., private communication.

[40] Houlberg, W.A., Shaing, K.C., Hirshman, S.P., and Zarnstorff, M.C., 1997 in *Phys. Plasmas* **4**, 3230.

[41] Ohkawa, T., 1997 in National Institute of Fusion Science, Research Report NIFS-484; Itoh, K., Ohkawa, T., Itoh, S.I., Yagi, M., and Fukuyama, A., "Role of Nonuniform Superthermal Ions for Internal Transport Barriers," in *Plasma Phys. and Contr. Nucl. Fusion Research* (Proc. IAEA Tech. Committee Mtg. US/Japan Wkshp. on H–Mode Physics, September 1997, Kloster Seeon, Germany), (IAEA, Vienna) to be published.

[42] Wong, S.K., 1987 in *Phys. Fluids* **30**, 818.

[43] Rogister, A.L., 1994 in *Plasma Phys. Control. Fusion* **36**, A213.

[44] Lin, Z., Tang, W.M., and Lee, W.M., 1995 in *Phys. Plasmas* **2**, 2975.

[45] Shaing, K.C., Hazeltine, R.D., and Zarnstorff, M.C., 1997 in *Phys. Plasmas* **4**, 771.

[46] Konings, J.A., and Waltz, R.E., 1997 in *Nucl. Fusion* **37**, 863.

[47] Hinton, F.L., 1985 in *Nuclear Fusion* **25**, 1457; Hinton, F.L., and Staebler, G.M., 1989 in *Nuclear Fusion* **29**, 405.

[48] Carlstrom, T.N., Burrell, K.H., and Groebner, R.J., "Comparison of a Grad-B Drift Effect Model with Measured Power Thresholds," in *Plasma Phys. and Contr. Nucl. Fusion Research* (Proc. IAEA Tech. Committee Mtg. US/Japan Wkshp. on H–Mode Physics, September 1997, Kloster Seeon, Germany), (IAEA, Vienna) to be published.

[49] Hassam, A.B., Antonsen, T.M., Drake, J.F., and Liu, C.S., 1991 in *Phys. Rev. Lett.* **66**, 312; Stringer, T.E., 1969 in *Phys. Rev. Lett.* **22**, 770.

[50] Staebler, G.M., and Dominguez, R.R., 1993 in *Nucl. Fusion* **33**, 77.

[51] Diamond, P.H., Liang, Y.-M., Carreras, B.A., and Terry, P.W., 1994 in *Phys. Rev. Lett.* **72**, 2565.

[52] Moyer, R.A., Burrell, K.H., Carlstrom, T.N., Coda, S., Conn, R.W., et al., 1995 in *Phys. Plasmas* **2**, 2397.

[53] Cornelis, J., Sporken, R., VanOost, G., and Weynants, R.R., 1994 in *Nucl. Fusion* **34**, 171.

[54] Kim, J., Burrell, K.H., Gohil, P., Groebner, R.J., Hinton, F.L., et al., 1994 in *Plasma Phys. Control. Fusion* **36**, A183.

[55] Monier-Garbet, P., Burrell, K.H., Hinton, F.L., Kim, J., and Garbet, X., et al., 1997 in *Nucl. Fusion* **37**, 403.

[56] Hinton, F.L., 1994 *Theory of Fusion Plasmas* [Int. School of Plasma Physics 'Piero Caldirola' (ISPP)] eds. E. Sindoni, et al., (Societa Italiana di Fisica, Bologna) p. 247

[57] Rozansky, V., and Tendler, M., 1992 in *Phys. Fluids B* **4**, 1877.

[58] Kim. J., private communication.

[59] Rozansky, V., and Tendler, M., 1994 in *Phys. Plasmas* **1**, 2711.